

P.85 Measurement Uncertainty and System Assessment for Weather Radar

Qing Cao¹, Michael Knight¹, Alexander Ryzhkov^{2,3}, and Pengfei Zhang^{2,3}

1: Research & Innovation, Enterprise Electronics Corporation (EEC), Enterprise, Alabama

*2: Cooperative Institute for Mesoscale Meteorological Studies (CIMMS), University of Oklahoma,
Norman, Oklahoma*

3: NOAA/National Severe Storms Laboratory (NSSL), Norman, Oklahoma

1. INTRODUCTION

With the widespread deployment of dual-polarization weather radars, data quality has become one of the major concerns for weather radar users worldwide. A well-designed and constructed radar system is a premise to acquire high quality radar data. In practice, measurement precision and system stability are primary questions to be answered for an operational weather radar system.

For weather radar, the measurement uncertainty can be discerned as the variation of radar moment estimates. Considering the random nature of the radar return from hydrometeors, the sampling effect is generally the major factor contributing to the statistical fluctuation of moment estimates. Here, this uncertainty is regarded as “sampling-induced uncertainty”. On the other hand, the system hardware imperfectness such as noise, instability, and other potential factors may cause the “system-induced uncertainty”. Previous literatures have mainly addressed the measurement uncertainty caused by the sampling effect (Bringi and Chandrasekar, 2001; Doviak and Zrnic, 1993; Melnikov, 2004). However, the uncertainty attributed to the system stability and quality has not routinely been a major focus. The sampling-induced uncertainty heavily relies on the data-sampling configuration of weather radar and is actually less related to the system itself. For

radar users, the system-induced uncertainty, which has less dependence on the sampling configuration, is of more importance for radar users to assess the quality of a radar system.

Recently, the Enterprise Electronics Corporation (EEC) has proposed a robust and easily implemented approach to quantify the measurement uncertainty of weather radar. The proposed approach applies the point mode scanning strategy and can quantify the measurement uncertainty more accurately than popular texture analysis method. More importantly, based on the data analysis, the system-induced uncertainty can be isolated from the total measurement uncertainty. As a result, it is particularly helpful for assessing the overall quality of an operational weather radar system. The current paper presents the theoretical basis and practical procedure of the proposed method and demonstrates its promising performance in quantifying the measurement uncertainty for weather radar system assessment.

2. MEASUREMENT UNCERTAINTY

The measurement uncertainty is usually characterized by the statistical fluctuation of radar moment estimates. Mathematically, the measurement uncertainty is quantified as a standard deviation (SD) of the estimates.

The sampling-induced uncertainty can be quantified based on the sampling theory of random hydrometeors measured by the weather radar (Melnikov, 2004). Assuming that radar echoes have a high signal-to-noise-ratio (SNR), the sampling-induced uncertainty

* Correspondence author address:
Dr. Qing Cao; 350 David L. Boren Blvd., Ste.
1780, Norman, OK 73072, U.S.A.
Email: qingcao@eecweathertech.com

of six radar moments: reflectivity (Z), radial velocity (V), spectrum width (W), differential reflectivity (Z_{DR}), differential phase (Φ_{dp}), and cross-correlation coefficient (ρ_{hv}) are given in the following formulas.

$$SD(Z) = 3.24(\sigma_{vn}M)^{-0.5} \quad (1)$$

$$SD(V) = \frac{\lambda}{T} \left(\frac{\sigma_{vn}}{32\sqrt{\pi}M} \right)^{0.5} \quad (2)$$

$$SD(W) = \frac{\lambda}{T} \left(\frac{3\sigma_{vn}}{128\sqrt{\pi}M} \right)^{0.5} \quad (3)$$

$$SD(Z_{DR}) = 4.62 \left(\frac{1-\rho_{hv}^2}{\sigma_{vn}M} \right)^{0.5} \quad (4)$$

$$SD(\Phi_{dp}) = 30.3 \left(\frac{\rho_{hv}^{-2}-1}{\sigma_{vn}M} \right)^{0.5} \quad (5)$$

$$SD(\rho_{hv}) = 0.53 \frac{1-\rho_{hv}^2}{(\sigma_{vn}M)^{0.5}} \quad (6)$$

where, $\sigma_{vn} = \frac{4WT}{\lambda}$

is the normalized spectrum width with a dimensionless unit, λ is the radar wavelength (in m), T is the pulse repetition period (PRT, in second), M is the number of pulses, and W is the Doppler spectrum width (in m/s). Eqs. (1-3) are adapted from Doviak and Zrnic (1993), whereas Eqs. (4-6) are taken from Melnikov (2004). These formulas are valid at high SNRs (>20dB). All the SD values are inversely proportional to the square root of the dwell time ($= M \times T$) of radar sampling. That is to say, the radar sampling with four times of dwell time would reduce 50% sampling-induced uncertainty. It is also worth noting that the SD values of polarimetric variables crucially depend on the magnitude of cross-correlation coefficient ρ_{hv} .

The objective of system assessment is to justify the quality of radar system. Since the sampling-induced uncertainty issue is quite fundamental, it can not give a comprehensive assessment of the system quality. Therefore, the system-induced uncertainty (due to system noise, instability, and other system imperfectness) becomes the most concerned

issue during the system assessment. However, the system-induced uncertainty is usually hard to be quantified through the radar data. Its quantification is seldom addressed in the literatures. In the next section, a novel method is proposed to quantify the system-induced uncertainty for the assessment purpose.

3. SYSTEM ASSESSMENT

This section presents a novel radar uncertainty assessment approach based on point-mode data collection/analysis strategy.

The point-mode surveillance means that the weather data are collected with the radar antenna pointing at one specific direction. It is reasonable to assume that the microphysics of precipitation in the same radial would keep the same within a very short time period (dwell time is only up to a couple of seconds). Therefore, similar to the error quantification through a side-by-side approach (Cao et al. 2008), the measurement error (standard deviation σ_x) can be quantified with two consecutive point-mode measurements (i.e., moment estimates), x_1 and x_2 , by Eqs. (7-9).

$$x_1 = \langle x \rangle + \varepsilon_1; \quad x_2 = \langle x \rangle + \varepsilon_2 \quad (7)$$

$$\langle |x_1 - x_2|^2 \rangle = \langle |\varepsilon_1 - \varepsilon_2|^2 \rangle = 2\sigma_x^2 \quad (8)$$

$$\sigma_x = \sqrt{0.5 \times \langle |x_1 - x_2|^2 \rangle} \approx \sqrt{0.5 \times |x_1 - x_2|^2} \quad (9)$$

where symbol “ $\langle \ \rangle$ ” indicates the expectation value. Parameter ε is the measurement error. Symbol “ $|\cdot|$ ” indicates the absolute value and symbol “ $\bar{\ \ }$ ” denotes the data averaging.

Eq. (7) assumes that the measurement x consists of the truth $\langle x \rangle$ and measurement error ε . Eq. (8) shows that the variance of $(x_1 - x_2)$, i.e., the difference between two consecutive measurements, should be twice as much as the variance of measurement error. Eq. (9) gives the estimate of σ_x using the data averaging, given the fact that the precipitation

process can be assumed to be an ergodic process.

It is worth noting that the measurement error estimated using Eq. (9) includes both system-induced error and sampling-induced error. The sampling-induced error needs to be excluded to better represent the quality of radar system. This can be accomplished through collecting two datasets with different sampling configurations.

The variance (σ_{data}^2) of measurement error for these two datasets can be written as

$$\begin{aligned}\sigma_{data1}^2 &= \sigma_{system}^2 + \sigma_{sampling1}^2 \\ \sigma_{data2}^2 &= \sigma_{system}^2 + \sigma_{sampling2}^2\end{aligned}\quad (10)$$

where subscripts “1” and “2” represent two different settings. The $\sigma_{sampling}^2$ indicates the variance of sampling-induced error. The σ_{system}^2 denotes the variance of radar system-induced error and should remain unchanged for both datasets.

As Eqs. (1-6) show, the $\sigma_{sampling}^2$ should be inversely proportional to the dwell time ($M \times PRT$) for data sampling. The ratio (m) of dwell time between two settings is given by

$$m = \frac{\sigma_{sampling1}^2}{\sigma_{sampling2}^2} = \frac{M_2 \times PRT_2}{M_1 \times PRT_1}\quad (11)$$

According to Eq. (10), the σ_{system}^2 values can be estimated by cancelling $\sigma_{sampling}^2$ as

$$\sigma_{system}^2 = (m\sigma_{data2}^2 - \sigma_{data1}^2)/(m - 1)\quad (12)$$

Therefore, in order to assess the radar system and data quality, the proposed method at least needs two consecutive point-mode measurements with the same sampling configuration and two datasets with different sampling configurations. Eq. (9) quantifies the variance of total measurement error of radar

data and Eq. (12) gives the variance of system-induced error.

4. DATA PROCESSING AND ANALYSIS

This section presents a case study to demonstrate the proposed method for radar data assessment.

The radar data used in this case study were collected by German Meteorological Service (DWD)’s C-band MHP radar at 10:25-11:10UTC on 29 July 2015. The storm feature is shown in Fig. 1 by PPI images of six radar moments (Z_H , Z_{DR} , ρ_{hv} , Φ_{dp} , W_h , and V_h).

The radar also used the point mode (i.e., the radar antenna stops rotating and points at fixed elevation and azimuth angles) for data collection during this period. The following two settings were used for collecting total 32 data files in the point-mode surveillance.

Setting one:

- PRF: 800Hz
- Pulse number 39
- Gate width 25 m
- Gate number 4800
- Elevation angle 0.5 °

Setting two:

- PRF: 300Hz
- Pulse number 255
- Gate width 25 m
- Gate number 4800
- Elevation angle 0.5 °

The major difference between these two settings is the dwell time used for radar moment estimation. The ratio of dwell time is

$$m = \frac{M_2 \times PRT_2}{M_1 \times PRT_1} = \frac{M_2 \times PRF_1}{M_1 \times PRF_2} = \frac{255 \times 800}{39 \times 300} = 17.436$$

The time intervals of two consecutive moment estimates in the same radial (fixed azimuth/elevation angles) are 0.05 second and 0.85 second for the first and second settings, respectively. Within such a short time interval, radar moments for two consecutive rays almost represent the same physics and

therefore their difference can well represent the true noise of moment estimates.

Figs. 2 and 3 give two examples of a-scope radar images for six raw radar moments (Z_H , Z_{DR} , ρ_{hv} , Φ_{dp} , W_h , and V_h). It is clearly seen that the dwell time difference for two settings causes different noisiness features in six radar moments. The first setting with a shorter dwell time of data collection apparently introduces more randomness, i.e., the radar data are noisier. The ρ_{hv} obtained with the first setting also has slightly decreased value, implying the degraded data quality attributed with the shorter dwell time.

The proposed radar data uncertainty assessment mentioned in sections 2 and 3 is based on the weather data with high SNRs. Therefore, the following data filtering criteria are utilized to find continuous precipitation region and precipitation data less affected by noise and non-hydrometeor contaminations.

- SNR>20 dB
- $\rho_{hv}>0.98$
- Texture of $\rho_{hv} >0.05$

The first threshold mitigates the noise effect. The second threshold ensures that most of signals are from precipitation. The third threshold is also helpful. It is known that the clutter returns might have very high ρ_{hv} values. The biographical-target-contaminated weather echoes might also satisfy the second threshold. Furthermore, heavily discontinuous region (with low ρ_{hv} values) in a precipitation region (with high ρ_{hv} values) implies the existence of unexpected contamination or abnormal degradation. Therefore, the third threshold is added to exclude these unwanted data. Considering the texture of ρ_{hv} in a continuous precipitation region is normally very small (<0.02), the third threshold may not bias the uncertainty quantification of precipitation data.

Figs. 4 and 5 show the histogram of moment difference (Δ) for radar data of two different settings. The Δ is x_1-x_2 , which is used

to calculate the standard deviation (σ_{data}) of radar data, as shown in Eq. (9). It is noted that the standard deviation of Δ is larger than measurement error and they have a relation of $\sigma_{\Delta} = \sqrt{2}\sigma_{data}$. As shown in Fig. 5, the Δ values for setting two clearly have much narrower distribution than the data for setting one, implying the setting two gives a much better data quality.

The table lists the standard deviation (SD) values estimated for four moments (Z_H , Z_{DR} , ρ_{hv} , and Φ_{dp}). The data points shown in Figs. 4 and 5 are used for the statistics in this table. In order to mitigate the statistical error caused by abnormal data points, the outliers that account for 1% of total data points have been excluded from the statistics.

As indicated in Eq. (10), measurement error consists of sampling-induced error and system-induced error. Because the sampling-induced error is dependent on precipitation physics, the error quantification in the table has been classified with four categories in terms of spectrum width (0.1-0.5 m/s, 0.5-1 m/s, 1-1.5 m/s, and 1.5-2 m/s). The results clearly show the measurement error decreases with increasing the spectrum width, as predicted by the theoretical results (Eqs. 1-6). The first four rows give the measurement errors quantified from the radar data collected with setting one. The next four rows give the measurement errors from the data of setting two. It is worth noting that these errors do not isolate the radar system-induced errors from sampling-induced errors. Using the data processing in Eqs. (10)-(12), the radar system-induced errors, shown in the bottom five rows, are estimated from the measurement errors listed in first eight rows.

As table 1 shows, the system-induced error is much less than the sampling-induced error (not listed in the table but can be implied by the total measurement error) for short dwell time data commonly collected in operational mode. The system error should be independent with the precipitation property and/or sampling effect. As shown in five

bottom rows, the system errors for four spectrum width categories are quite consistent although the $SD(Z)$ has a minor exception for this case. The consistency within the system error estimates matches the expectation.

For MHP radar system, the estimated system errors for Z_H , Z_{DR} , ρ_{hv} , and Φ_{dp} measurements are 0.4664 dB, 0.0419 dB, 0.0020, and 0.3522 degree, respectively. These numbers are much smaller than the quality requirements (1 dB, 0.1 dB, 0.005, and 1 degree), which are recommended by DWD for operational systems. Regardless of the sampling-induced error, the small system error implies that MHP radar could produce reliable measurements.

5. CONCLUSION

This study proposes a novel method for assessing the quality of weather radar system. It is shown that the measurement uncertainty of weather radar can be ascribed to two types: sampling-induced and system-induced. The sampling-induced uncertainty normally has a major effect on the quality of radar data. However, it is less meaningful to radar system assessment because it is only determined by the sampling configuration of radar operation and the property of measured weather. The reasonable radar system assessment may require the quantification of system-induced uncertainty.

The proposed method is based on the processing/analysis of weather data collected in radar surveillance with the point-mode. The data with different sampling settings can help to exclude the sampling-induced error from the total measurement error so that the system-induced error can be quantified. The

detailed procedure of error quantification is demonstrated with a case study using a C-band polarimetric weather radar system. The data analysis shows reasonable error results quantified for this weather radar system.

In short, the proposed method can be used as an effective tool for the system assessment of weather radars.

ACKNOWLEDGMENT

The authors would like to thank Dr. Michael Frech and his colleagues at German Meteorological Service (DWD), who have helped with the radar experiments for this study.

REFERENCES

- Bringi, V.N. and V. Chandrasekar, 2001: Polarimetric Doppler Weather Radar: Principles and Applications. *Cambridge University Press*, 648 pp.
- Cao, Q., G. Zhang, E. Brandes, T. Schuur, A. Ryzhkov, and K. Ikeda, 2008: Analysis of Video Disdrometer and Polarimetric Radar Data to Characterize Rain Microphysics in Oklahoma. *J. Appl. Meteor. Climatol.*, 47, 2238–2255.
- Doviak, R.J. and D.S. Zrnic, 1993: Doppler Radar and Weather Observations. *Academic Press*, San Diego, CA.
- Melnikov, Valery M., 2004: "Simultaneous Transmission Mode for the Polarimetric WSR-88D: Statistical Biases and Standard Deviations of Polarimetric Variables", NOAA/NSSL Report, 84 pages. (available at: http://www.nssl.noaa.gov/publications/wsr88d_reports/SHV_statistics.pdf)

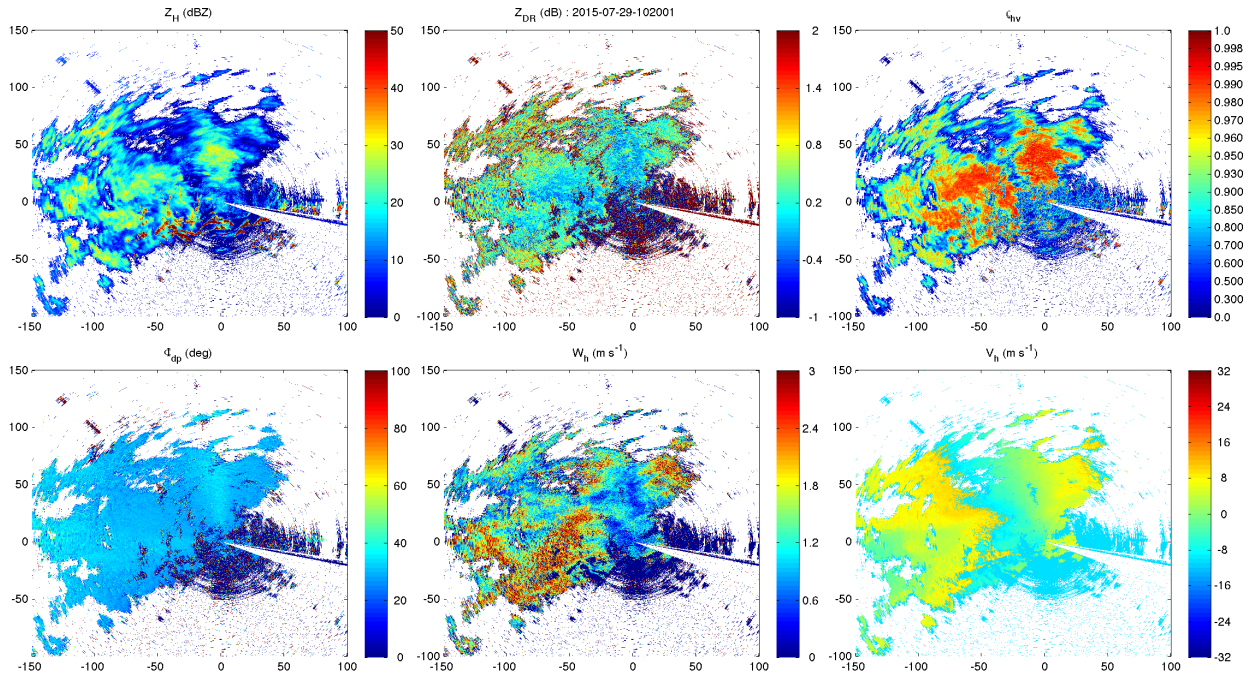


Figure 1. PPI images of raw data of Z_H , Z_{DR} , ρ_{hv} , Φ_{dp} , W_h , and V_h (from left to right, top to bottom) collected by C-band MHP radar (10:20:01UTC, 29 July 2015).

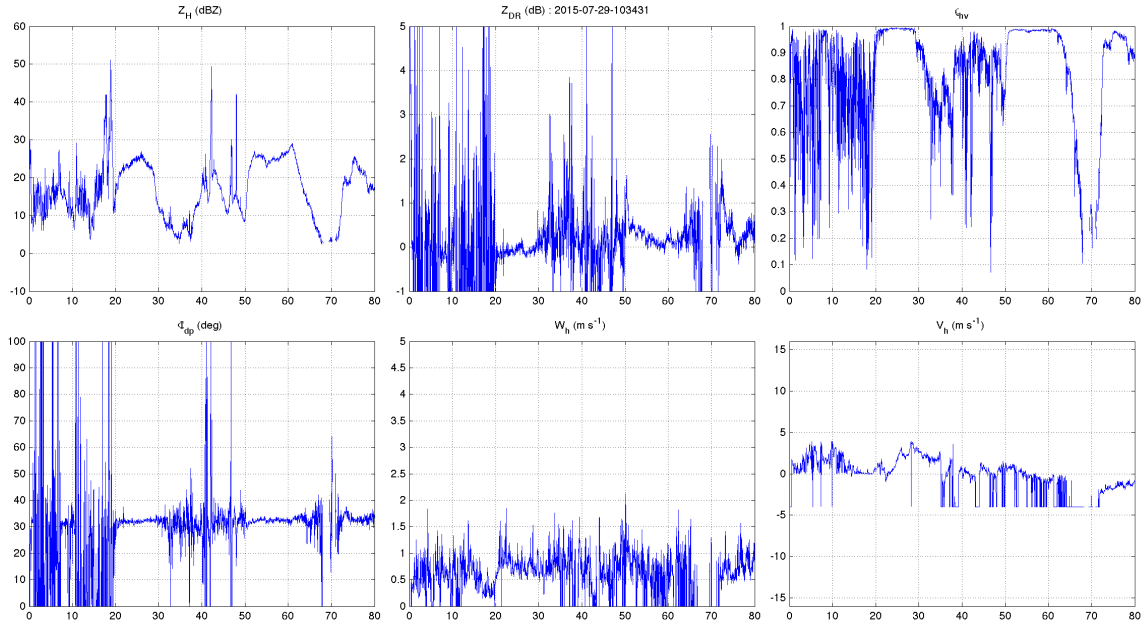


Figure 2. A-scope of raw data of Z_H , Z_{DR} , ρ_{hv} , Φ_{dp} , W_h , and V_h (from left to right, top to bottom) collected by C-band MHP radar using setting one (10:34:31UTC, 29 July 2015).

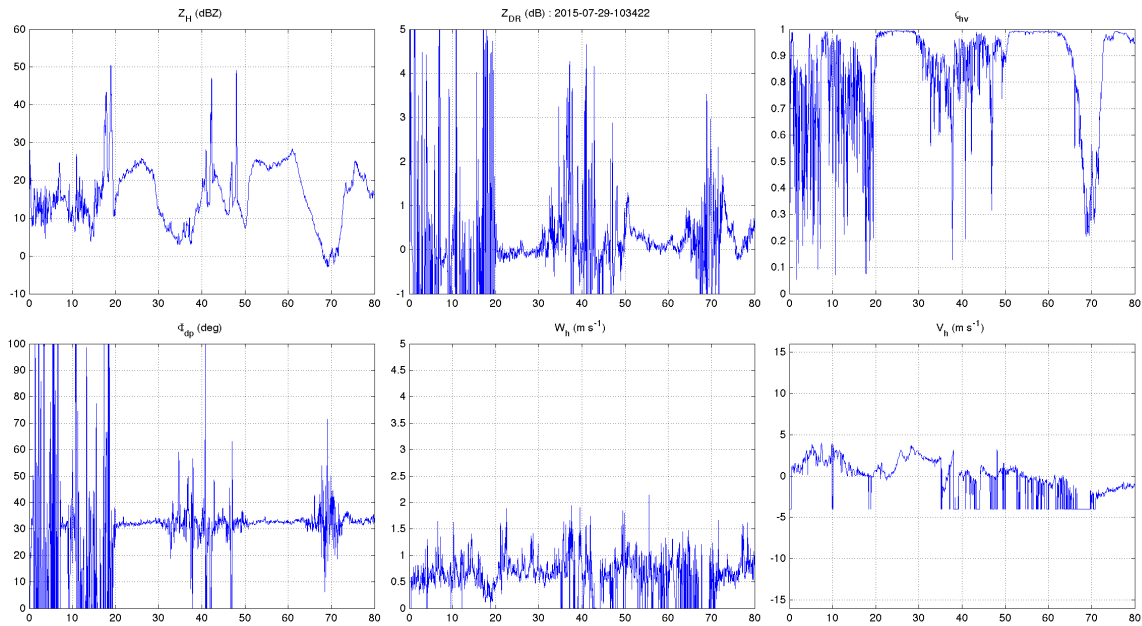


Figure 3. The same as Fig. 2 except for setting two (10:34:22UTC, 29 July 2015).

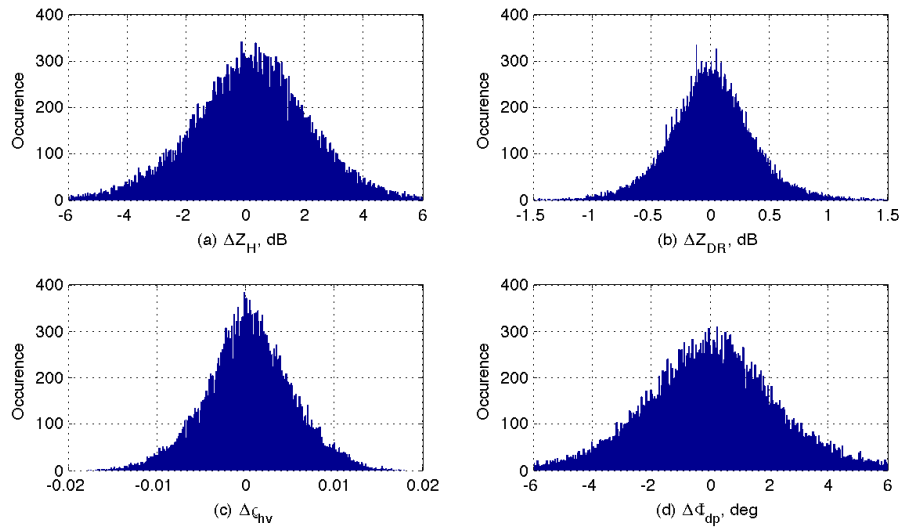


Figure 4. The histogram of moment differences between two consecutive rays: (a) $\Delta Z_{H'}$, (b) $\Delta Z_{DR'}$, (c) $\Delta \rho_{hv}$, and (d) $\Delta \Phi_{dp}$. The data were collected with setting one and limited by $0.1 < W < 2$ m/s.

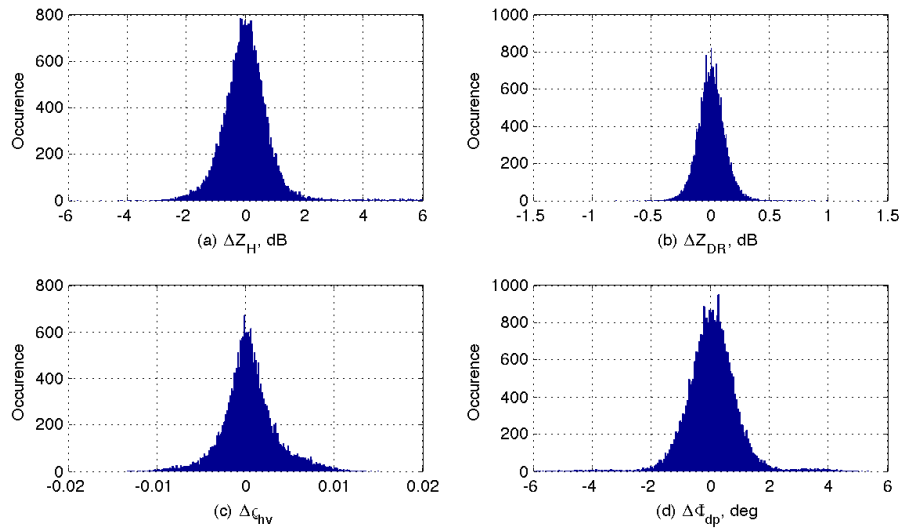


Figure 5. The same as Fig. 4 except for setting two.

Table: Statistics of SD values for four radar moments (event 07/29/2015)

Datasets	Criteria for Data Filtering	SD(Z_H)	SD(Z_{DR})	SD(ρ_{hv})	SD(Φ_{dp})	Data Points
Setting One (pulse_number=39, PRF=800Hz)	$\rho_{hv}>0.98$ & $0.5>W>0.1$ m/s	1.673	0.310	0.0036	2.050	7140
	$\rho_{hv}>0.98$ & $1>W>0.5$ m/s	1.550	0.273	0.0036	1.867	23496
	$\rho_{hv}>0.98$ & $1.5>W>1$ m/s	1.366	0.229	0.0033	1.545	22123
	$\rho_{hv}>0.98$ & $2>W>1.5$ m/s	1.185	0.184	0.0030	1.228	15269
Setting Two (pulse_number=255, PRF=300Hz)	$\rho_{hv}>0.98$ & $0.5>W>0.1$ m/s	0.726	0.086	0.0022	0.588	5080
	$\rho_{hv}>0.98$ & $1>W>0.5$ m/s	0.691	0.074	0.0020	0.572	18629
	$\rho_{hv}>0.98$ & $1.5>W>1$ m/s	0.501	0.068	0.0020	0.525	5515
	$\rho_{hv}>0.98$ & $2>W>1.5$ m/s	0.375	0.062	0.0021	0.431	582
Estimated System Error	$\rho_{hv}>0.98$ & $0.5>W>0.1$ m/s	0.6232	0.0443	0.0021	0.3330	
	$\rho_{hv}>0.98$ & $1>W>0.5$ m/s	0.6002	0.0366	0.0019	0.3671	
	$\rho_{hv}>0.98$ & $1.5>W>1$ m/s	0.3906	0.0415	0.0019	0.3837	
	$\rho_{hv}>0.98$ & $2>W>1.5$ m/s	0.2516	0.0454	0.0020	0.3250	
Mean System Error		0.4664	0.0419	0.0020	0.3522	